Drugs in R&D (2024) 24:285–301
https://doi.org/10.1007/s40268-024-00471-9

ORIGINAL RESEARCH ARTICLE

Demonstration of Physicochemical and Functional Similarity of Biosimilar Pegfilgrastim-cbqv to Pegfilgrastim

Henriette Kuehne[1] · Janice M. Davis[1] · LeeAnne Merewether[1] · Matthew McQueen[1,2] · Elizabeth Valentine[1,3] · Glen Young[1] · Benjamin T. Andrews[1,4] · Dimitri Diaz[1,2] · Karen J. Miller[1]

Accepted: 6 June 2024 / Published online: 3 July 2024

Abstract

Background Pegfilgrastim-cbqv/CHS-1701 (UDENYCA®) (hereafter referred to as pegfilgrastim-cbqv) was approved in 2018 by the US Food and Drug Administration as a biosimilar for pegfilgrastim (Neulasta®) (hereafter referred to as pegfilgrastim). Both pegfilgrastim-cbqv and pegfilgrastim are conjugates of recombinant human granulocyte colony stimulating factor (r-metHuG-CSF) with a 20 kDa polyethylene glycol (PEG) indicated to decrease the incidence of infection, as manifested by febrile neutropenia, in patients receiving myelosuppressive anticancer drugs. The demonstration of analytical similarity for PEG-protein conjugates presents unique challenges since both the protein and PEG attributes must be characterized.

Objective The current study demonstrates the analytical similarity of pegfilgrastim-cbqv and the reference product, pegfilgrastim. In addition to the physicochemical and functional characterization of the protein, the study assessed attributes specific to PEGylation including PEG size and polydispersity, site of attachment, linker composition, and PEGylation process-related variants.

Methods The structural, functional, and stability attributes of pegfilgrastim-cbqv and pegfilgrastim were compared using state-of-the-art analytical methods. For the protein, the primary structure, disulfide structure, and secondary and tertiary structures were assessed using traditional protein characterization techniques such as mass spectrometry (MS), circular dichroism (CD), intrinsic fluorescence, and differential scanning calorimetry (DSC), as well as more advanced techniques such as two-dimensional (2D) nuclear magnetic resonance (NMR) and hydrogen deuterium exchange (HDX). For the PEG moiety, the site of attachment, occupancy, linker composition, size and polydispersity were compared using mass spectrometry (both intact and after endoprotease digestion), multiangle light scattering detection (MALS), and Edman degradation. Purity assessments included the assessment of both protein variants and PEGylation variants using chromatographic and electrophoretic analytical separation techniques. The functional similarity between pegfilgrastim-cbqv and pegfilgrastim was compared using both a cell-based bioassay and surface plasmon resonance (SPR). The degradation rates and stability profiles were compared under accelerated and stressed conditions.

Results Biosimilarity was demonstrated by a thorough assessment of physiochemical and functional attributes, as well as comparative stability, of pegfilgrastim-cbqv relative to pegfilgrastim. These studies demonstrated identical primary structure and disulfide structure, highly similar secondary and tertiary structure, as well as functional similarity. The impurity profile of pegfilgrastim-cbqv was comparable to that of pegfilgrastim with only minor differences in PEGylation variants and a slight offset in the PEG molar mass. These differences were not clinically relevant. The degradation profiles were qualitatively and quantitatively similar under accelerated and stress conditions.

Conclusion The structural, functional, and stability data demonstrate that pegfilgrastim-cbqv is highly similar to the reference product, pegfilgrastim.

1 Introduction

Biosimilars are biological products that have been demonstrated to be highly similar to a licensed biological product (reference product). Biosimilars lower health care costs by introducing competition to the marketplace [1]. In the USA, the BPCI Act of 2009 created an abbreviated pathway for licensure for biosimilars, as outlined in specific guidance documents [2–4]). These guidances require biosimilar products to demonstrate that they are "highly similar to the

Extended author information available on the last page of the article

Key Points

Biosimilars require extensive testing to demonstrate structural and functional attributes are comparable with those of the reference products. Pegfilgrastim contains both a protein and a PEG moiety that must be assessed.

The extensive comparative analysis presented here was key to the US approval of pegfilgrastim-cbqv as a biosimilar to pegfilgrastim.

Minor differences in PEGylation variants and a slight offset in the PEG molar mass did not impact the overall conclusion of similarity between pegfilgrastim-cbqv and pegfilgrastim.

reference product notwithstanding minor differences in clinically inactive components" [2]. Comparative analytical studies are the foundation for this demonstration of similarity.

Pegfilgrastim-cbqv was approved by the FDA in 2018 as a biosimilar to pegfilgrastim, based upon both clinical and comparative analytical studies. Since its launch, pegfilgrastim-cbqv has been administered to over 300,000 patients [5] with a current cost savings of 35% per dose versus pegfilgrastim [6]. Pegfilgrastim-cbqv is the only biosimilar pegfilgrastim available in three presentations: a prefilled syringe, an autoinjector [7], and an on-body injector [8]. Clinical studies demonstrated that pegfilgrastim-cbqv has pharmacokinetic and pharmacodynamic equivalence [9] as well as similar immunogenicity [10] to pegfilgrastim. The analytical and functional studies used to demonstrate similarity are presented here.

The analytical comparability of pegfilgrastim to pegfilgrastim-cbqv presents unique challenges due to the presence of the 20 kDa poly(ethylene) glycol (PEG) covalently bonded to the N-terminus of the filgrastim protein. In addition to characterization of the filgrastim protein, the comparative analytical assessment evaluated PEG attributes including the linker composition, site of attachment, PEG size, and PEG heterogeneity. This paper describes studies demonstrating pegfilgrastim-cbqv as highly similar to pegfilgrastim, as determined by a thorough assessment of each product's physiochemical, functional, and stability attributes. The differences observed were minor and not clinically relevant.

2 Materials and Methods

2.1 Materials

Structural and functional assessments were performed on up to 13 independent lots of pegfilgrastim-cbqv drug product and up to 22 lots of commercially available US pegfilgrastim drug product (NEULASTA®, pegfilgrastim). Both products are formulated in 10 mM acetate, 5% sorbitol, 0.004% polysorbate 20, pH 4.

2.2 Methods

2.2.1 Statistical Approach

Quantitative results were subjected to statistical comparisons of pegfilgrastim-cbqv to the reference product pegfilgrastim to establish whether acceptance criteria were met. Statistical analyses were carried out using one of two approaches, based on risk ranking of the product quality attributes. Following the approach developed by an FDA working group [11], the most critical quantitative attributes with highest risk to clinical outcome were compared using an equivalence test and the quantitative attributes with a lesser risk to clinical outcome were compared using quality ranges. Quantitative results and statistical analyses are provided (Online Resource 1).

The equivalence test was based on standard deviation and confidence intervals derived from the results generated on reference product lots. Equivalence is shown if the 90% two-sided confidence interval of the difference between means for pegfilgrastim and pegfilgrastim-cbqv falls within the equivalence acceptance criterion of ± 1.5 standard deviations (σ) based on the σ calculated from tested pegfilgrastim lots. Calculation of the 90% confidence interval was performed limiting the degrees of freedom to reflect no more pegfilgrastim lots than 1.5 times the number of pegfilgrastim-cbqv lots. Unequal variances were assumed.

For attributes assessed using quality ranges, similarity is shown if results for at least 90% of pegfilgrastim-cbqv lots (12 of 13) are within the one-sided or two-sided limits, as appropriate. The quality range is defined as the mean $\pm k \times \sigma$ with $k = 2.3$ for two-sided criteria and mean + or - $k \times \sigma$ with $k = 1.9$ for one-sided criteria, where σ is the standard deviation of the pegfilgrastim values. The k values for these quality ranges were determined using a Monte Carlo simulation. To represent the values from pegfilgrastim, 17–22 random values from a standard normal distribution (mean of 0 and standard deviation of 1) were generated. A quality range was then calculated from these 17–22 values using a prespecified value of k, i.e., mean $\pm k\sigma$ for two-sided specifications and mean $+ k\sigma$ for one-sided specifications. To represent the values from pegfilgrastim-cbqv, 13 random values from a standard normal distribution were generated. The number of values from the simulated pegfilgrastim-cbqv data that met the quality range established from the simulated pegfilgrastim lots at a specific k value was then calculated. This simulation was repeated with 100,000

iterations and the percentage of times that 12 out of the 13 simulated pegfilgrastim-cbqv lots met the quality range established from the simulated pegfilgrastim lots was determined. This full simulation was performed adjusting the *k* values until the percentage of times that 12 out of 13 lots met the quality range criteria was 90%.

2.2.2 Analytical Methods

The methods used for the comparative analytical assessment are described in the following sections. These methods were qualified and shown to be fit for purpose (data not shown). The pegfilgrastim-cbqv primary reference standard lot was used as the reference standard for all functional testing for which relative activity was used to assess similarity. Pegfilgrastim-cbqv samples were analyzed side by side with reference product samples wherever possible.

2.2.2.1 Reduced and Nonreduced Peptide Mapping with Liquid Chromatography–Tandem Mass Chromatography (LC–MS/MS) Samples were digested with endoproteinase GluC and analyzed both nonreduced and reduced by dithiothreitol (DTT). Peptides were separated on a Waters ACQUITY UPLC Peptide BEH C18 column using a water/acetonitrile gradient containing 0.05% trifluoroacetic acid. Effluent was directed from the ultraviolet (UV) detector into a Waters Q-TOF mass spectrometer with positive electrospray ionization. Data were analyzed using Waters BiopharmaLynx software (version 1.2).

2.2.2.2 Edman Sequencing Sequencing was performed by analyzing 500 pmole of sample on an Applied Biosystems 494HT Procise N-terminal protein sequencer per manufacturer's instructions. Samples were sequenced for ten or more cycles/residues.

2.2.2.3 Intact Mass Intact mass was measured using a Waters Q-TOF (quadrupole time of flight) mass spectrometer coupled to a Waters ACQUITY UPLC. A 0.5% solution of *N*,*N*-diethylmethylamine (DEMA) in 50% acetonitrile was added to the sample postcolumn to reduce the charge on the PEG molecules [12, 13] and allow deconvolution. Data were deconvoluted using Waters MaxENT1 (version 4.1) with a mass window from 38,000 to 43,000 Da. The resulting spectra show a distribution of masses due to the polydispersity of the PEG moiety. Estimated values for weight average molar mass (M_w), number average molar mass (M_n), and polydispersity index (M_w/M_n) were calculated using the mass values and intensity values from the deconvoluted spectra M_w and M_n are calculated as follows:

$$M_w = \Sigma M_i^2 N_i / \Sigma M_i N_i$$

$$M_n = \frac{\Sigma M_i N_i}{\Sigma N_i},$$

where M_i represents individual mass values and N_i represents individual intensity values, as a surrogate for individual number values.

2.2.2.4 PEG Linker Analysis Samples were digested with trypsin. The PEG-containing peptide was isolated by RPC using a Sepax Bio-C18 5 µm 300 Å 10×250 mm column and a linear acetonitrile/TFA gradient. The peak of interest was collected and concentrated by vacuum centrifugation. The collected and concentrated PEG peptide samples were analyzed using the MS procedure for intact mass.

2.2.2.5 Circular Dichroism (CD) Samples were diluted with formulation buffer (10 mM acetate, 5% sorbitol, 0.004% polysorbate 20, pH 4) to 1 mg/ml. CD measurements were carried out at room temperature on a Jasco J-715 spectropolarimeter using a 1 cm cell for near-UV CD and a 0.02 cm cell for far-UV CD. After subtracting the buffer spectrum, the CD spectrum of each sample was converted to the mean residue ellipticity (CD intensity per amino acid) using the nominal protein concentration, the mean residue weight (average weight per amino acid) of 107.4, and the path length of the cell.

2.2.2.6 Fluorimetry Intrinsic tryptophan fluorescence spectrum was collected on a Horiba Fluormax-4 fluorimeter. Samples were diluted with formulation buffer to a final concentration of 0.1 mg/ml before data collection. Excitation was at 280 nm and intrinsic fluorescence data were collected in the range of 280–450 nm. The excitation and emission slit widths were both 5 nm, and the scan rate was 300 nm/min.

2.2.2.7 Differential Scanning Calorimetry (DSC) DSC was performed using a Malvern VP-Capillary DSC. The sample and reference cells were loaded with degassed sample (diluted to 0.5 mg/ml) and formulation buffer, respectively. The instrument was programmed to scan from 10 to 105 °C, at a rate of 60 °C/h. The *Cp* profiles were normalized to protein concentration.

2.2.2.8 2D Nuclear Magnetic Resonance (NMR) Sample volumes of 500 µl were diluted with 20 µl D_2O and 15 µl 4,4-dimethyl-4-silapentane-1-sulfonic acid (DSS). 1D NMR and 2D Nuclear Overhauser Enhancement spectroscopy (NOESY) data were acquired on 600 MHz and 700 MHz Bruker instruments equipped with a cryoprobe. Sam-

ple temperature was 300K. Presaturation was used to suppress the very large peaks from polyethylene glycol.

2.2.2.9 Hydrogen Deuterium Exchange Samples were exchanged in D_2O for 10 s, 1 min, 12 min, 60 min, or 240 min at 20 °C. Following exchange, samples were quenched by addition of a denaturing guanidine solution. Quenched samples were digested with pepsin, then the resulting peptides were separated using a C18 column and a linear gradient. The separated peptides were analyzed using an LTQ-Orbitrap mass spectrometer. Data were analyzed to determine the percentage of deuterium uptake (%D) of each peptide at each time point.

2.2.2.10 Potency by Proliferative Bioassay Potency was measured based on induction of the proliferation of NFS-60 cells, a murine myeloblastic cell line infected with Cas Br-M murine leukemia virus that is dependent on G-CSF for growth and maintenance of viability in vitro. Proliferation is detected through use of thiazolyl blue tetrazolium bromide (MTT), a yellow tetrazole that is reduced to purple formazan in living cells. The amount of formazan generated is directly proportional to the number of living cells.

2.2.2.11 Receptor Binding by Surface Plasmon Resonance Binding studies were performed using a Biacore T200 label-free optical biosensor. Recombinant hG-CSFR was coupled to the sensor surface at three different surface densities using standard amine coupling chemistry. The samples were tested for binding to the receptor surfaces at four discrete concentrations spanning a ~30-fold concentration range [from ~1.4 to ~37 ng/ml (0.07–2.0 nM)] at 25 °C with one concentration [~4 ng/ml (0.2 nM)] injected in duplicate (five sample injections total). Response data from the three different density surfaces and five injections were globally fit to extract association and dissociation rates and calculate binding constants. Raw data from the three densities and five injections were used to generate a single affinity result.

2.2.2.12 Size-Exclusion Chromatography with UV, RI, and MALS Detection SEC utilized a Sepax SRT SEC-300 column, 5 µm particle size, at 7.8×300 mm. Isocratic elution was performed in a mobile phase of 100 mM sodium phosphate pH 6.5 with 5% ethanol at a column temperature of 25 °C. Absorbance at 280 nm was measured with a UV detector, RI was recorded using a Wyatt Optilab T-rEX, and multiangle light scattering detection (MALS) on a Wyatt MiniDAWN TREOS or DAWN HELEOS. Molar mass calculations using Wyatt Astra software (version 6) were performed using a 280 nm extinction coefficient value of 0.86 ml/mg/cm. A protein d*n*/d*c* value of 0.180 and a PEG d*n*/d*c* value of 0.134 was used based on standard values adjusted for the ethanol content in the mobile phase [14], where *n* is the refractive index and *c* is the solute concentration.

2.2.2.13 SDS–PAGE (Silver Stain) Samples were diluted with water, LDS sample buffer (4×, Invitrogen), and NuPAGE Sample Reducing Agent (10×, Invitrogen, for reduced gels only) as needed to achieve the desired load of 1 µg per well. Samples were heated for 10 min at 70 ºC. Ten µl of each sample was loaded on a NuPAGE 4–12% Bis–Tris 1.0 mm Gel, 12 well/17 well (Invitrogen). Running buffer was prepared by dilution of MOPS SDS Running Buffer (20×, Invitrogen) with purified water. Electrophoresis was carried out at a constant voltage of 200 V, 120 mA for 50 min. The gels were stained with silver (SilverXpress, Invitrogen).

2.2.2.14 Reversed Phase Chromatography Samples were analyzed using a binary Thermo Dionex Ultimate 3000 HPLC, a Restek Viva C18 250 mm × 4.6 mm, 5 µm, 300 Å column at 60 °C, and a water/acetonitrile gradient containing 0.1% trifluoroacetic acid. Detection was by absorbance at 215 nm.

2.2.2.15 Cation Exchange Chromatography Samples were analyzed using a quaternary Thermo Dionex Ultimate 3000 HPLC, a TSKgel SP-NPR column at 35 °C, and a salt gradient using mobile phases of 10 mM acetic acid, pH 4.75 with 5% ethanol and 10 mM acetic acid plus 400 mM NaCl, pH 4.75. Detection was by absorbance at 280 nm.

2.2.2.16 Isoelectric Focusing with Silver Stain Gel IEF was performed on a Serva HPE BlueHorizon flatbed system using FocusGel pH 3–7 gels. A 5 µg sample was loaded into prepolymerized sample wells at the cathode end of the gel. Electrophoretic focusing was carried out at 550 V, 20 mA, and 10 W for 30 min for sample entrance, followed by 2000 V, 20 mA, and 30 W for ~3.5 h for band sharpening. The gel was fixed for 1 h. Silver staining was used to visualize bands (Serva silver staining kit for native PAGE). pI standards were included both as reference and to confirm proper separation.

2.2.2.17 Microflow Imaging Subvisible particulate (SVP) concentration was measured by microflow imaging (MFI) using a ProteinSimple MFI 5200. Samples were expelled from syringes into a 5 ml clean glass vial and degassed under light vacuum prior to analysis. Images were filtered to exclude silicon oil by removing particulate images with an aspect ratio of ≥ 0.85.

2.2.2.18 Protein Concentration by UV Spectrophotometry Protein concentration was measured using a CTech™ SoloVPE® variable pathlength spectrophotometer. Absorb-

ance was measured at 280 nm with an extinction coefficient of 0.86 ml/mg/cm.

2.2.3 Comparative Stability Studies

The relative stability of pegfilgrastim-cbqv and pegfilgrastim were compared by a variety of stability-indicating analytical methods under accelerated storage conditions (25 °C) and several different stressed stability conditions, including light exposure, oxidation, acidic, basic, and heat stress (40 °C) conditions. For the accelerated stability studies, three lots each of pegfilgrastim and pegfilgrastim-cbqv are presented. Samples were tested at 0-, 1-, 3-, and 6-month time points. For heat stressed stability, three lots each of pegfilgrastim and pegfilgrastim-cbqv were incubated at 40 °C in parallel. Samples were tested at 0-, 1-, 2-, and 3- month time points.

3 Results

State-of-the-art physiochemical and functional assays were used to evaluate all relevant quality attributes of pegfilgrastim-cbqv and reference product considering the physicochemical characteristics of both the protein and PEG components, as well as the mechanism of action. Comparative stability studies at accelerated and stress conditions were used to compare degradation rates and degradation profiles. A summary of the comparative analytical assessment results is presented in Table 1.

3.1 Primary Structure

The primary structures of pegfilgrastim-cbqv and reference product were evaluated using complementary techniques, including peptide mapping with LC-MS/MS, N-terminal sequencing by Edman degradation, and intact mass analysis.

3.1.1 Peptide Mapping with LC/MS-MS

Reduced Glu-C peptide map profiles of pegfilgrastim-cbqv and reference product were highly similar by visual assessment (Fig. 1a). MS/MS analysis (data not shown) confirmed that all pegfilgrastim-cbqv and pegfilgrastim lots tested matched the theoretical sequence; however, the N-terminal peptide (residues 1–20) could not be assessed due to the PEG moiety attached to the N-terminal peptide (Fig. 1b). A comparison of nonreduced peptides by LC–MS with the corresponding reduced peptides confirms that the expected disulfide bonds, Cys37–Cys43 and Cys65–Cys75, are present (Fig. 1c). Nonreduced peptide maps of pegfilgrastim-cbqv and pegfilgrastim were also highly similar by visual assessment (Fig. 1d). Overall, the peptide mapping data confirms that pegfilgrastim-cbqv and pegfilgrastim contain the same amino acid sequence (excluding the N-terminal residues) and the same disulfide structure (Table 1).

3.1.2 N-terminal Sequence and PEG Occupancy

Edman sequencing was used to compare PEG occupancy at the N-terminal methionine as well as to confirm the N-terminal sequence, which could not be identified by peptide mapping with MS/MS detection as discussed earlier. Edman sequencing detects amino-acid residues in order, starting at the N-terminus; however, if the N-terminus is PEGylated, the first residue (methionine) is not observed [15]. Instead, the second residue in the sequence (threonine) is the first residue detected. The first residue (methionine) is only detected for molecules without N-terminal PEG. Therefore, relative levels of methionine detected compared to the total amount of protein loaded can provide an estimate of the unoccupied N-terminal PEGylated site. The major sequence detected for all lots analyzed was Thr–Pro–Leu–Gly–Pro–Ala–Ser–Ser–Leu–Pro, indicating that the N-terminal methionine is blocked, presumably by the PEG group. A minor methionine signal is detected in the first cycle, at approximately 1% of the theoretical 500 pmol load for both pegfilgrastim-cbqv and pegfilgrastim. Edman sequencing data demonstrate that the N-termini of pegfilgrastim-cbqv and pegfilgrastim both contain the expected amino acid sequence and less than 1% of both products are unPEGylated at the N-terminal methionine residue (Table 1).

3.1.3 Intact Mass

Intact mass was used to assess PEG mass and polydispersity and to confirm the overall covalent structure of pegfilgrastim-cbqv compared with pegfilgrastim. Polydispersity is a parameter used for polymers to describe the width of a size distribution. For both products, a range of masses separated by 44 Da [the mass of a single ethylene glycol (EG) subunit within the PEG] and centered on approximately 40 kDa is observed (Fig. 2a). This finding is consistent with an r-met-Hu-G-CSF mass of 18.8 kDa plus a polydisperse PEG moiety averaging approximately 21 kDa. An offset is observed with the M_n values for pegfilgrastim-cbqv, which are slightly larger than that of pegfilgrastim (Fig. 2a and Table 1).

PEG molar masses for pegfilgrastim-cbqv and pegfilgrastim (net masses after subtracting the expected mass of the protein moiety) differ by less than 2%. The difference in molar mass is likely due to different sources of PEG (different vendor and different batches) used to manufacture each product.

While PEG size is directly correlated to in vivo half-life, only substantial differences (on the order of tens of percent) in PEG size are expected to make a meaningful impact

Table 1 Comparative structural and functional analytical assessment results

Quality attribute	Method	Lots, pegfilgrastim: pegfilgrastim-cbqv	pegfilgrastim-cbqv range	pegfilgrastim range	Acceptance criterion[a]	Results
Primary structure						
Amino acid sequence and PEG occupancy	Peptide map with LC–MS/MS	22:13	Pegfilgrastim-cbqv reduced map matched pegfilgrastim by visual assessment. Pegfilgrastim-cbqv sequence and pegfilgrastim matched the expected sequence			Met
	N-terminal sequence by Edman degradation	22:13	Pegfilgrastim-cbqv and pegfilgrastim matched expected sequences. UnPEGylated N-terminus (methionine signal) was ~ 1% for both materials			Met
Disulfide structure	Nonreduced Glu-C peptide map with LC–MS/MS	22:13	Pegfilgrastim-cbqv nonreduced map matched pegfilgrastim by visual assessment. The correct disulfides are present (Cys37–Cys43, Cys65–Cys75).			Met
Intact mass (M_n)	LC–MS	16:13	40,269.4–40,310.7	39,926.2–39,979.5	39,9921.3–39,993.1	Not met[b]
Polydispersity		16:13	All values for pegfilgrastim-cbqv and pegfilgrastim were 1.0002 demonstrating similar polydispersity within assay capability			Met
PEGylated peptide mass analysis: PEG size, heterogeneity, and PEG linker		1:1	Individual species within mass spectra overlap with minor differences in relative abundance indicating the PEG-protein linkers likely have the same atomic composition, but different average PEG size			Not Met[b]
Higher-order structure						
Secondary and tertiary structures	Far and near UV CD	20:13	CD spectra similar between pegfilgrastim-cbqv and pegfilgrastim by visual comparison			Met
Tertiary structure	Intrinsic fluorescence	20:13	Fluorescence spectra similar between pegfilgrastim-cbqv and pegfilgrastim by visual comparison			Met
Tertiary structure and thermal stability	DSC	20:13	DSC curves similar between pegfilgrastim-cbqv and pegfilgrastim by visual comparison.			Met
Secondary and tertiary structures	2D NOESY NMR	17:13	NMR spectra similar between pegfilgrastim-cbqv and pegfilgrastim by visual comparison			Met
Tertiary structure	HDX	3:3	Uptake plots similar between pegfilgrastim-cbqv and pegfilgrastim by visual comparison			Met
Functional activity						
Biological activity (potency)	Proliferative bioassay	22:13	92–105 Observed 90% CI of the difference between means of − 1.0 to 3.5	92–103	90% CI of the difference between means within ± 5.6	Met
Receptor binding	SPR, K_D (pM)	20:13	62–157	78–155	68–166	Met
Purity and impurities						
Size variants, % HMW	SE-HPLC	22:13	0.5–1.0	1.3–1.6	≤ 1.6	Met
Size variants, % main peak			98.9–99.5	98.3–98.7	≥ 98.3	Met
Size variants, % LMW			< 0.1	< 0.1–0.1	≤ 0.1	Met
Size variant characterization, main peak M_w (kDa)	SEC-MALS	22:13	38.7–39.7	38.7–40.9	38.2–40.4	Met

Table 1 (continued)

Quality attribute	Method	Lots, pegfilgrastim: pegfilgrastim-cbqv	pegfilgrastim-cbqv range	pegfilgrastim range	Acceptance criterion[a]	Results
Hydrophobicity variants, % prepeaks	RP-HPLC	22:13	0.3–0.9	0.5–1.2	≤1.2	Met
Hydrophobicity variants, % main peak			98.3–99.0	95.9–97.1	≥95.8	Met
Hydrophobicity variants, % postpeaks			0.6–0.9	2.3–3.2	≤3.3	Met
DiPEGylated variants, %	CEX-HPLC	22:13	0.3–0.8	0.3–0.4	≤0.5	Not met
Deamidated species, %			All values < 0.1	0.1–0.3	≤0.3	Met
Main peak, %			99.1–99.8	99.3–99.5	≥99.3	Not met
General properties						
SVPs, count/ml[c] (≥2-µm range)	MFI	20:13	639–4419	2251–18,971	≤18,622	Met
SVPs, count/ml[c] (≥10-µm range)			3–47	9–109	≤103	Met
SVPs, count/ml[c] (≥25-µm range)			0–6	0–19	≤12	Met
Protein concentration (mg/ml)	UV absorbance at 280 nm	22:13	9.6–10.1	9.8–10.1	90% CI of the difference between means within ±0.11	Met
			Observed 90% CI of the difference between means of −0.10 to 0.05			

[a]Twelve of thirteen pegfilgrastim-cbqv lots must fall with the quality ranges

[b]Slight offset likely due to differences in the PEG raw material used in manufacturing

[c]Nonsilicone droplet or air bubble, aspect ratio ≤0.85 for 2, 10, and 25 µm or more particles

CEX-HPLC cation exchange high performance liquid chromatography, *CD* circular dichroism, *CI* confidence interval, *DSC* differential scanning calorimetry, *ELISA* enzyme-linked immunosorbent assay, *HDX* hydrogen deuterium exchange, *HMW* high molecular weight, K_D equilibrium dissociation constant, *LC–MS/MS* liquid chromatography with tandem mass spectrometry, *LC–MS* liquid chromatography with mass spectrometry, *LMW* low molecular weight, *MFI* microflow imaging, M_n number average molar mass, M_w weight average molar mass, *NOESY* nuclear overhauser effect spectroscopy, *NMR* nuclear magnetic resonance, *PEG* polyethylene glycol, *SE-HPLC* size-exclusion chromatography, *RP-HPLC* reversed phase high performance liquid chromatography, *SPR* surface plasmon resonance, *SVP* subvisible particles, *UV* ultraviolet

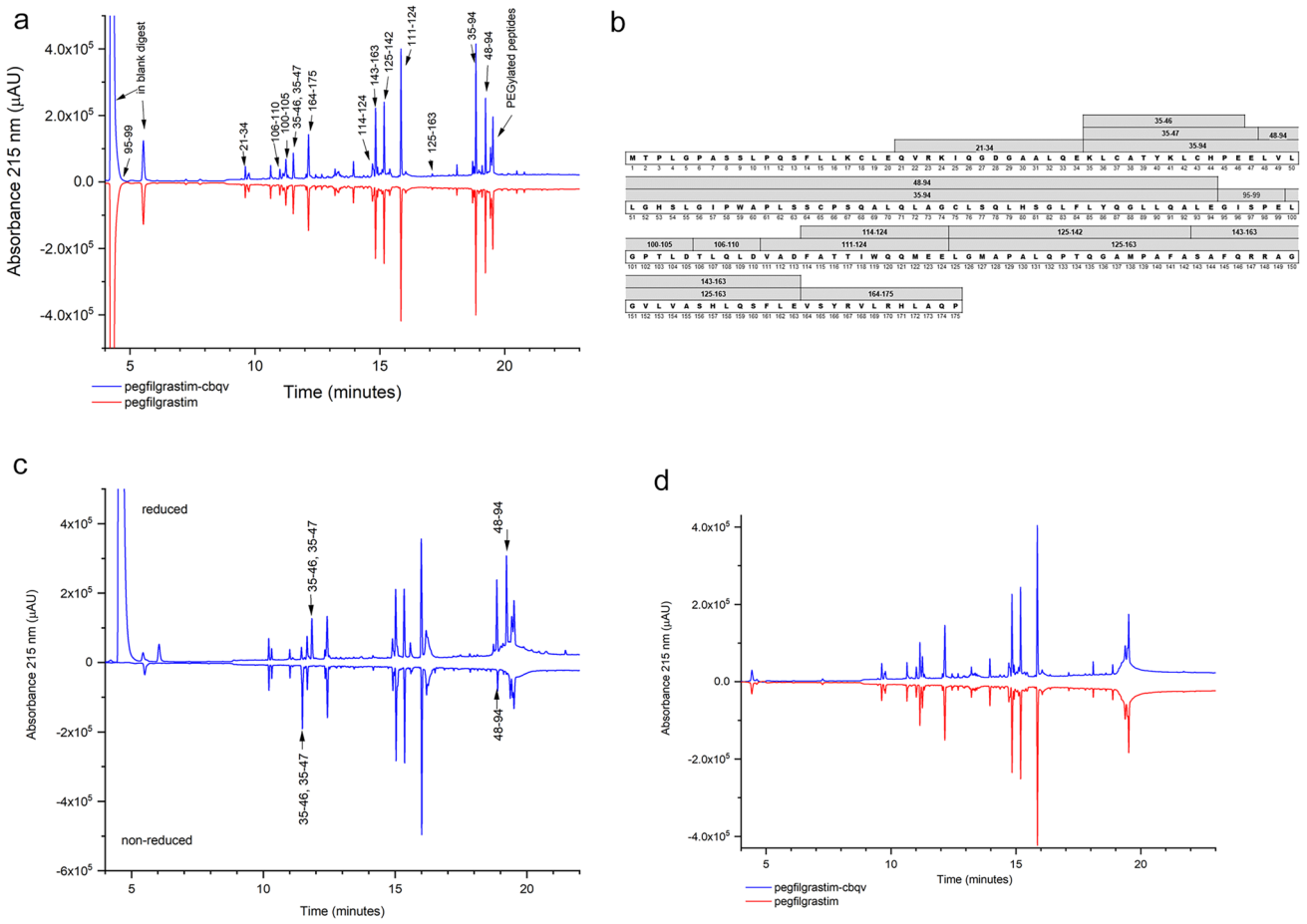

Fig. 1 Primary structures analyses comparing **a** reduced Glu-C peptide maps of representative pegfilgrastim-cbqv and pegfilgrastim lots with peptides labeled, **b** filgrastim amino acid sequence showing sequence coverage, **c** reduced and nonreduced Glu-C maps with the disulfide-containing peptides labeled for a representative pegfilgrastim-cbqv lot, and **d** nonreduced Glu-C peptide maps of representative pegfilgrastim-cbqv and pegfilgrastim lots

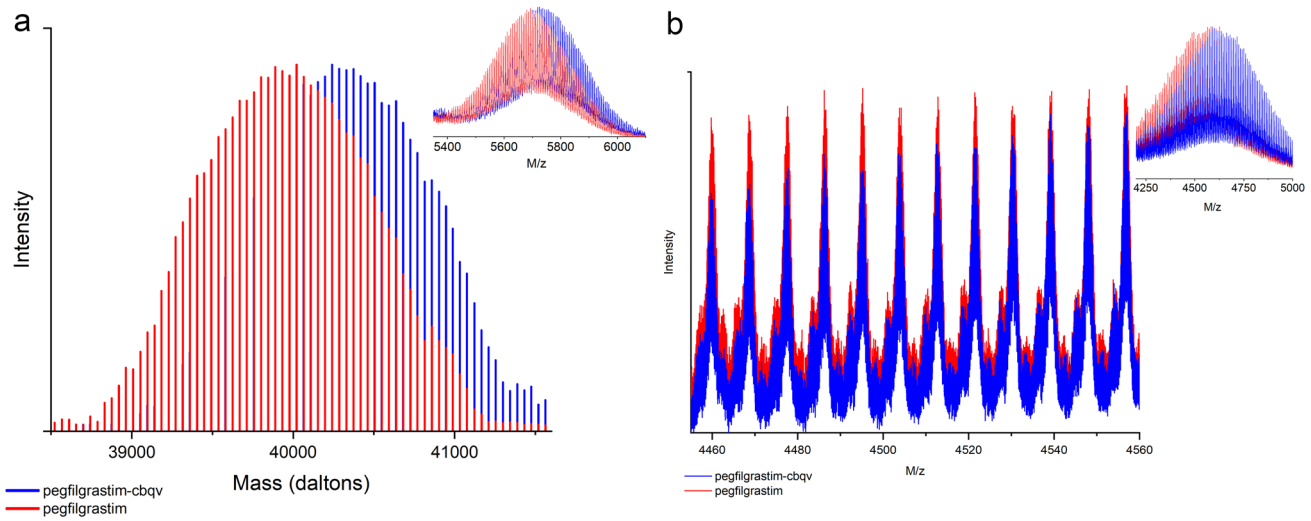

Fig. 2 Mass spectra from representative pegfilgrastim-cbqv and pegfilgrastim **a** deconvolved centroid spectra with raw spectra of +7 charge state in inset and **b** PEG-containing N-terminal peptides +5 charge state enlarged to show overlap of individual peaks with full spectra in inset

[16]. The small difference observed here did not result in clinical differences in pharmacokinetic (PK) attributes, as pegfilgrastim-cbqv was found to be bioequivalent in clinical studies [9].

In addition to intact mass analysis of pegfilgrastim-cbqv and pegfilgrastim lots, the N-terminal tryptic peptide (Met1 to Lys17) containing the PEG group was analyzed by LC–MS analysis using the same technique as for the intact mass of the PEGylated protein (Fig. 2b). The individual mass-to-charge ratios (m/z) are a good match between pegfilgrastim-cbqv and pegfilgrastim. The finding that the individual mass peaks within the polydispersity envelope line up exactly indicates that the PEG-protein linkers in pegfilgrastim-cbqv and pegfilgrastim likely have the same atomic composition. The only observed difference between the pegfilgrastim-cbqv and pegfilgrastim materials is a slight shift in the relative abundances of the individual species with different numbers of EG subunits, due to slight differences in average PEG size, as discussed earlier.

3.2 Secondary and Tertiary Structure

Near-UV CD, far-UV CD, and native fluorescence were used to evaluate the secondary and tertiary structures of pegfilgrastim-cbqv and pegfilgrastim. Spectra were within experimental variability, confirming that the solution structures are highly similar (Fig. 3a–c).

DSC monitors a protein's unfolding transitions in response to temperature changes, which are indicative of tertiary structure and structural stability. The DSC curves of pegfilgrastim-cbqv and pegfilgrastim indicate that the two molecules are highly similar (Fig. 3d).

NMR analyses were carried out to further compare the solution structures of pegfilgrastim-cbqv and pegfilgrastim. Nuclear Overhauser effect spectroscopy (NOESY) spectra show the through-space interactions between proximal nuclei regardless of whether they are connected by chemical bonds. NOESY is useful in protein structure examinations since molecules with the same fold should display the same NOESY patterns. 2D ^{1}H–^{1}H NOESY results over the full spectral range are visually comparable for pegfilgrastim-cbqv and pegfilgrastim (Fig. 3e).

Similarity of the tertiary structure, surface accessibility and dynamics of pegfilgrastim-cbqv and pegfilgrastim was confirmed using HDX (Fig. 4). Deuterium exchange of backbone amide protons in a protein depends on their solvent accessibility, local structure (e.g., hydrogen bonding), and the dynamics of the region studied, with faster exchange indicating more solvent-accessible regions. The deuterium uptake plot (Fig. 4) illustrates that the overall pattern of solvent accessibility is similar.

3.3 Biological Activity and Receptor Binding

The primary mechanism of action of G-CSF is stimulation of progenitor cell proliferation, decreased maturation of postmitotic precursor cells and mobilization of neutrophil storage pools from bone marrow. The cell-based proliferation assay, which measures the biological activity of the molecule based on its induction of the proliferation of NFS-60 cells, reflects key functional properties of G-CSF. The relative potency of pegfilgrastim-cbqv and pegfilgrastim met the equivalence acceptance criteria (Table 1). The dose/response curves for the two materials also demonstrate a similar response in the proliferation assay within assay variability (Fig. 5a).

The functional comparability of pegfilgrastim-cbqv to pegfilgrastim was also assessed by measuring the binding affinity to the G-CSF receptor using surface plasmon resonance (SPR). The quality-range acceptance criterion for the equilibrium dissociation constant (K_D) of pegfilgrastim-cbqv was met (Table 1). Sensorgrams for representative pegfilgrastim-cbqv and pegfilgrastim lots show similar binding curves with rapid binding and very slow dissociation (Fig. 5b).

3.4 Purity and Impurities

The purity of pegfilgrastim-cbqv and pegfilgrastim were assessed with respect to size variants, hydrophobicity variants, and charge variants. The data are presented with the minor species identified, if known. Minor species were identified by first isolating each peak and then applying characterization techniques such as Size Exclusion Chromatography with Multi-Angle Light Scattering (SEC-MALS), intact mass spectrometry (MS), and/or peptide mapping with mass spectrometry. The characterization data supporting peak identification are not shown, but are generally consistent with the minor species that have previously been identified in filgrastim (e.g., methionine oxidation [17, 18]), glutamine deamidation [19] or PEGylation variants known to result from the conjugation process (e.g., diPEGylated species or unPEGylated species [20]).

3.4.1 Size Variants

Size-exclusion high-performance liquid chromatography (SE-HPLC) was used to assess the relative abundance of both higher and lower molecular weight species. For PEGylated proteins, higher molecular weight species may include large oligomers, undesirable due to their potential for immunogenicity, as well as covalent species such as diPEGylated monomer. Low molecular weight (LMW) species include unPEGylated monomer (G-CSF) and

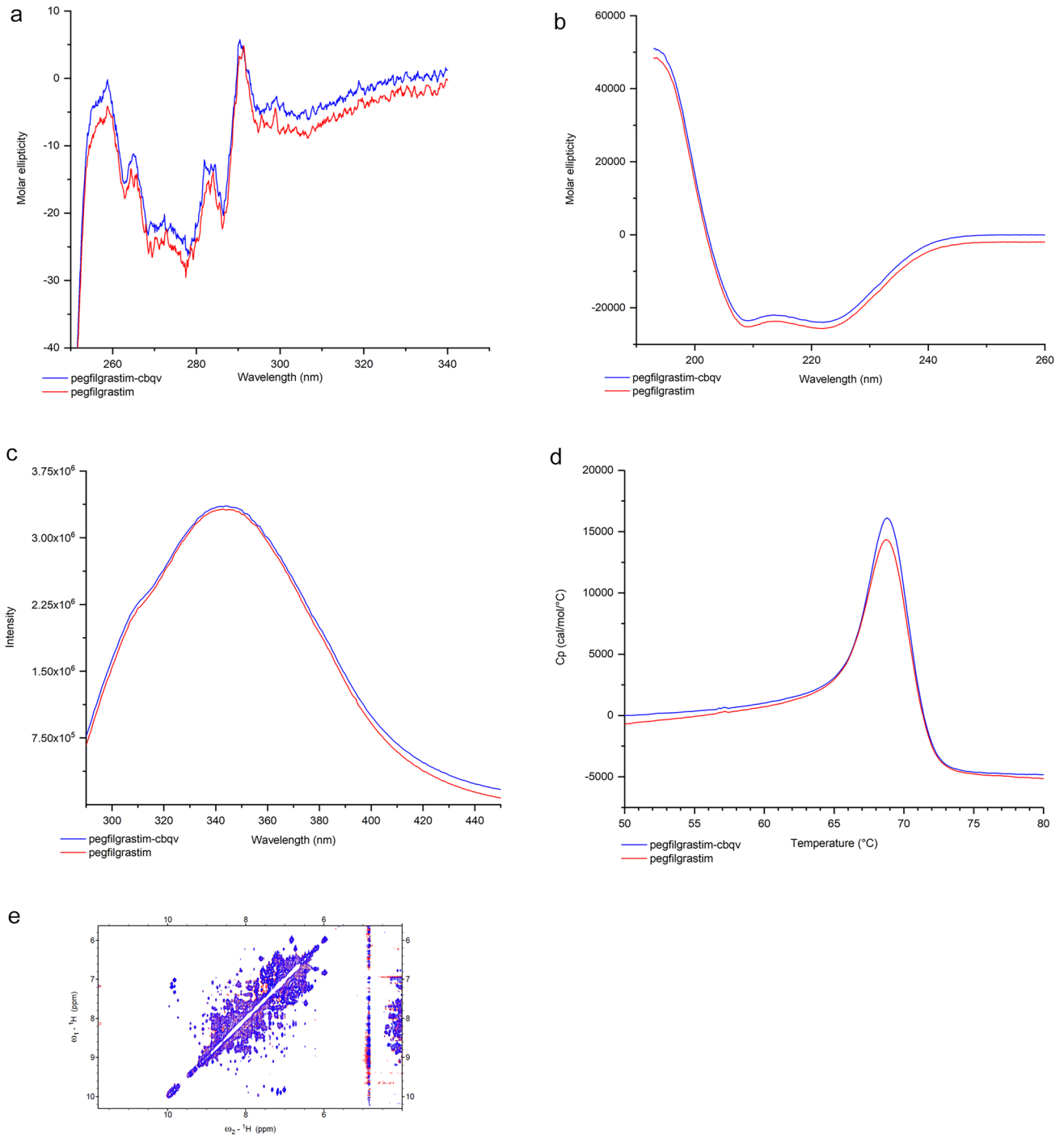

Fig. 3 Higher order structural analyses from representative pegfilgrastim-cbqv and pegfilgrastim lots **a** near-UV CD, **b** far-UV CD, **c** fluorescence, **d** DSC, and **e** 2D NOESY NMR. *CD* circular dichroism, *DSC* differential scanning calorimetry, *NOESY* nuclear overhauser effect spectroscopy, *NMR* nuclear magnetic resonance

clips, which could impact pharmacokinetics if present at high levels. Size-exclusion chromatograms of representative pegfilgrastim-cbqv and pegfilgrastim lots, with peaks labeled, are shown in Fig. 6a. Pegfilgrastim-cbqv appears more homogeneous than pegfilgrastim. Three early and one late eluting peak are observed in pegfilgrastim. In addition, pegfilgrastim shows an elevated baseline trough between the dimer/diPEG and main peaks that is absent in pegfilgrastim-cbqv. Only dimer/diPEG is present at quantifiable levels in pegfilgrastim-cbqv lots. The one-sided

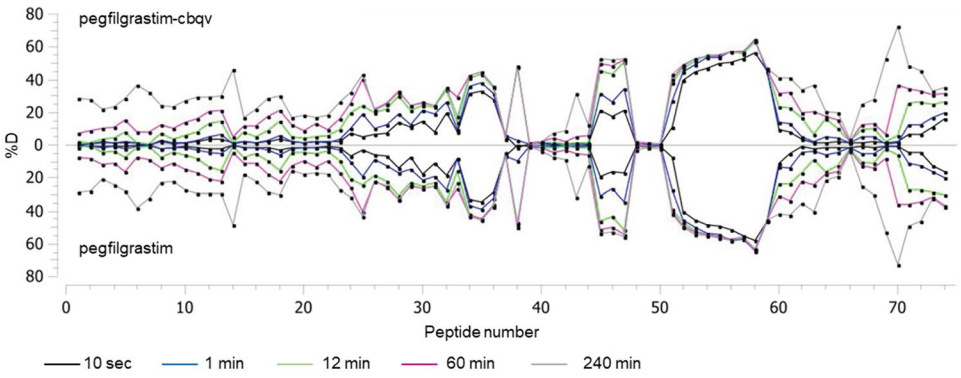

Fig. 4 Hydrogen/deuterium exchange uptake plots for representative pegfilgrastim-cbqv and pegfilgrastim lots. Results are presented as a measure of percent deuterium exchange compared with total number of protons for each individual peptide generated in a pepsin digest, numbered from the N-terminus to the C-terminus. Exchange time points are plotted as individual lines

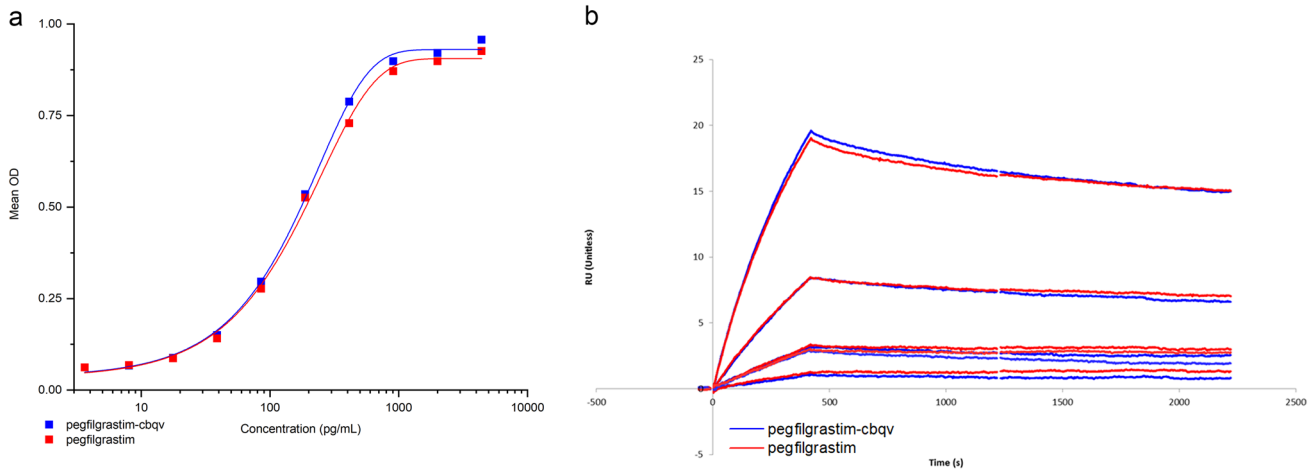

Fig. 5 Functional analyses for representative pegfilgrastim-cbqv and pegfilgrastim lots **a** dose/response curves for cell-based proliferation assay and **b** SPR sensorgrams for binding to G-CSFr at different product concentrations [from ~ 1.4 to ~ 37 ng/ml (0.07–2.0 nM)]. *SPR* surface plasmon resonance, *G-CSFr* granulocyte colony stimulating factor receptor

similarity criteria were met for higher and lower molecular weight species as well as main peak by SE-HPLC (Table 1).

SEC with in-line UV, refractive index (RI), and multiangle light scattering (MALS) detection provides additional characterization of comparability with respect to size. SEC-MALS with both UV and RI detectors to monitor protein and conjugate concentration, respectively, confirms the weight average molar mass (M_w) of the main species. Light scattering and UV chromatograms of pegfilgrastim-cbqv and pegfilgrastim with calculated molar mass values for selected peaks, are shown in Fig. 6b. The M_w of the main peaks are comparable between pegfilgrastim-cbqv and pegfilgrastim (Table 1). The slight difference in M_w observed by mass spectrometry was not detected by the lower-resolution MALS technique.

The most prominent minor peak in both pegfilgrastim-cbqv and pegfilgrastim is the dimer/diPEG peak, eluting just before the main peak. Characterization data show that both dimers of monoPEGylated species (dimer, ~ 80 kDa) and diPEGylated species (one protein with two PEG or one PEG of 2× size, ~ 60 kDa) elute in the same peak (data not shown). The observed M_w and the relative area for the dimer/diPEG peak are both significantly higher in pegfilgrastim, suggesting a greater proportion of dimers and higher multimers compared to pegfilgrastim-cbqv. The abundance of species eluting prior to the dimer/diPEG peak is too low for molar mass determination by MALS in these samples.

Sodium dodecyl sulfate–polyacrylamide gel electrophoresis (SDS–PAGE) with silver staining provides a useful visual comparison of the relative size and distribution of the species present in pegfilgrastim-cbqv and pegfilgrastim under denaturing conditions (Fig. 6c, d). Both pegfilgrastim-cbqv and pegfilgrastim contain a major band between the 64 kDa and 51 kDa marker bands, plus a minor higher-molecular-weight band near the 97 kDa marker (likely the diPEGylated species). PEGylated proteins are known to have decreased electrophoretic mobility relative to unPEGylated proteins

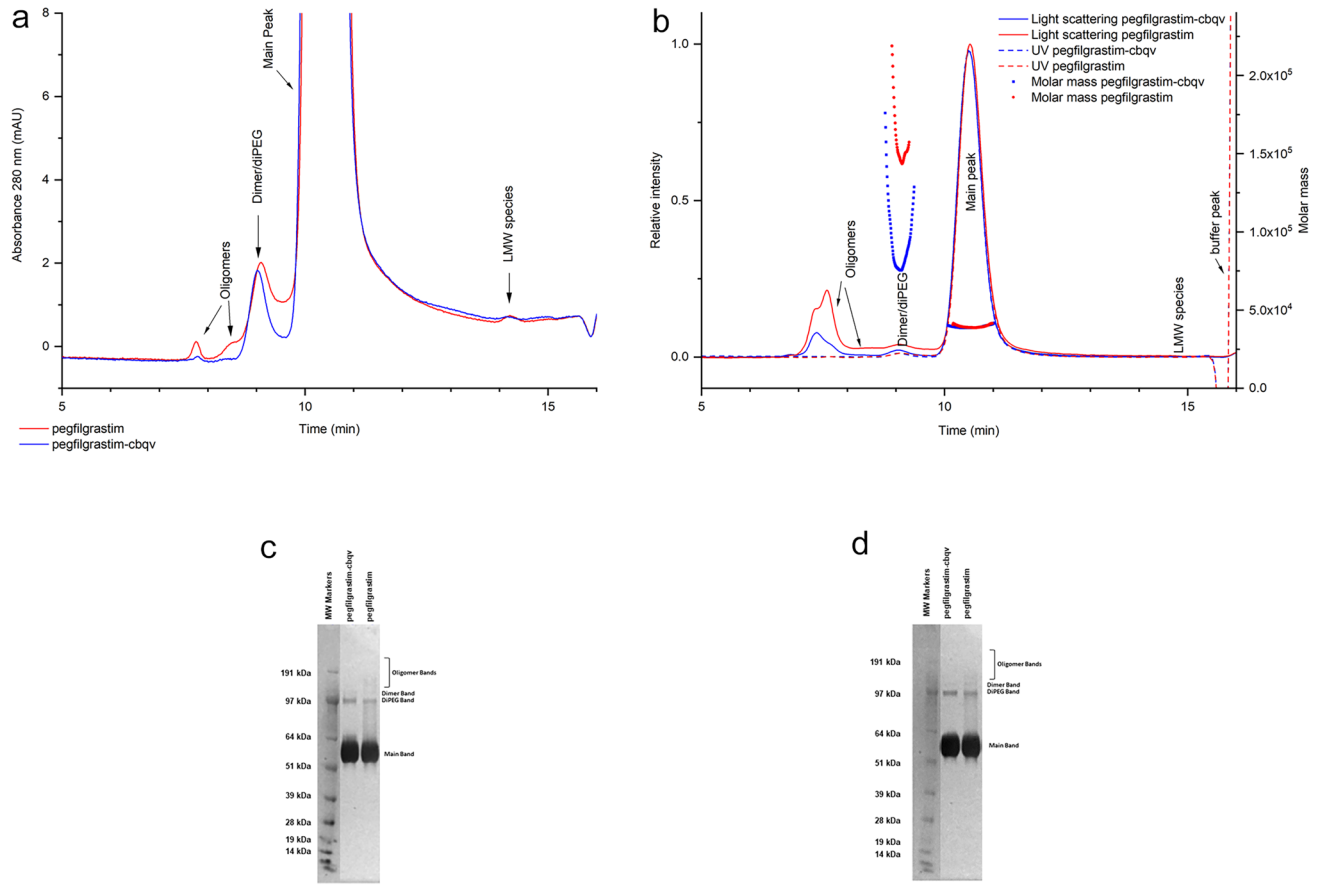

Fig. 6 The size variants of representative pegfilgrastim-cbqv and pegfilgrastim lots as assessed by **a** SE-HPLC with UV detection, **b** SE-HPLC with MALS detection—molar mass shown on the right axis and UV and light scattering shown on the left axis, **c** reduced SDS–PAGE with silver-stain, and **d** nonreduced SDS–PAGE with silver-stain. *SE-HPLC* size-exclusion high-performance liquid chromatography, *MALS* multiangle light scattering, *SDS–PAGE* sodium dodecyl sulfate–polyacrylamide gel electrophoresis

of corresponding size [21]. Pegfilgrastim also shows faint bands at higher apparent molecular weight than the diPEG band under nonreducing conditions, along with diffuse intensity between the diPEG and main bands in both reduced and nonreduced gels. These features are not observed in the pegfilgrastim-cbqv lots. This finding is consistent with the observation of a trough between the dimer/diPEG and main peaks by SE-HPLC. The gel images demonstrate that both products have similar size and distribution for the main band and the largest of the minor bands, the diPEGylated species, with pegfilgrastim-cbqv demonstrating a slightly more homogeneous distribution.

3.4.2 Hydrophobicity Variant

Reversed phase chromatography (RPC) was used to separate product variants, including oxidized and deamidated species, on the basis of hydrophobicity. RPC chromatograms of representative pegfilgrastim-cbqv and pegfilgrastim lots with peaks labeled are shown in Fig. 7a. Oxidized species, which elute as prepeaks, and deamidated species, which elute as postpeaks, are both lower in pegfilgrastim-cbqv than in pegfilgrastim. The one-sided similarity criteria were met for total prepeaks, main peak, and total postpeaks by RPC (Table 1).

3.4.3 Charge Variants

Cation exchange chromatography (CEC) was used to evaluate the similarity of pegfilgrastim-cbqv and pegfilgrastim with respect to charge variants, which include PEGylation variants as well as deamidated species (Fig. 7b). Monomers with double-sized PEG at the amino terminus, if present at high levels, could have the potential to affect pharmacokinetics, since a significantly larger PEG has been associated with somewhat greater in vivo activity, as well as somewhat diminished in vitro activity [16]. DiPEGylated species, in addition to potential effects on PK, may diminish activity if the second PEGylation site is near the G-CSF receptor binding site. For deamidated species, the impact on

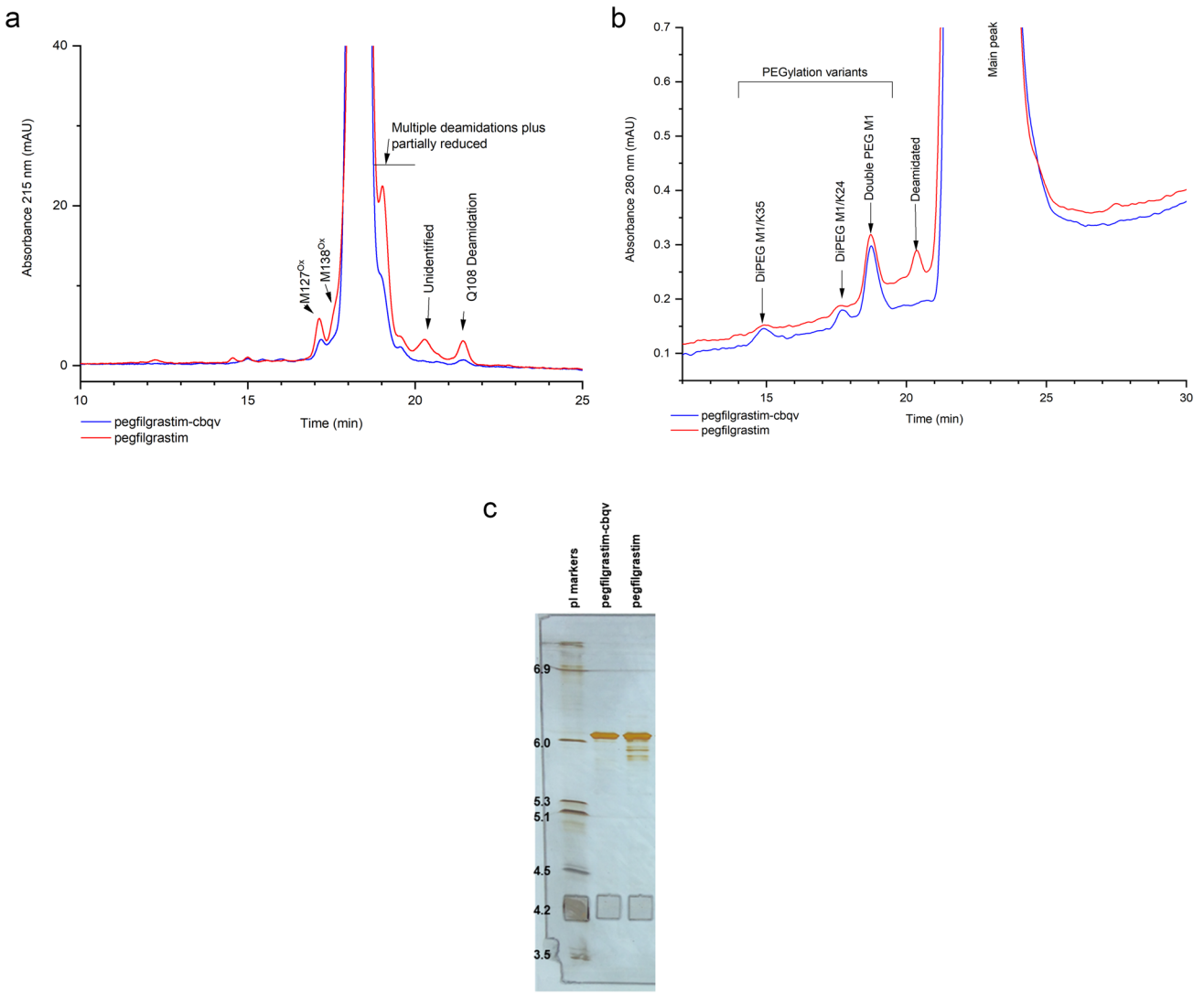

Fig. 7 Purity of representative pegfilgrastim-cbqv and pegfilgrastim lots using **a** RP-HPLC, **b** CEX-HPLC, and **c** IEF. *RP-HPLC* reversed-phase high-performance liquid chromatography, *CEX-HPLC* cation exchange high-performance liquid chromatography, *IEF* isoelectric focusing

activity is also site specific. The deamidated species peak is absent in pegfilgrastim-cbqv, while the diPEGylated peaks (diPEG M1/K35 and diPEG M1/24) are slightly larger in pegfilgrastim-cbqv. The acceptance criteria were not met for diPEGylated species and main peak (Table 1). However, diPEGylation variants are well under 1% for both pegfilgrastim-cbqv and pegfilgrastim, and no clinical impact was observed from these minor differences.

Isoelectric focusing (IEF) provided a qualitative comparison of the primary isoelectric point of pegfilgrastim-cbqv and pegfilgrastim, along with an assessment of charge homogeneity. The apparent isoelectric point of all pegfilgrastim-cbqv and pegfilgrastim lots analyzed was similar, as indicated by the alignment of the main bands (Fig. 7c), providing additional confirmation of the structure with respect to charged residues. Minor bands are more abundant in pegfilgrastim consistent with the higher levels of deamidation observed by RPC and CEC.

3.5 General Properties

3.5.1 Subvisible Particles

Subvisible particles, which may include potentially immunogenic protein particles, were evaluated using microflow imaging (MFI). Since samples are extracted from prefilled syringes, silicone oil droplets can dominate the particle counts. To minimize the contribution of

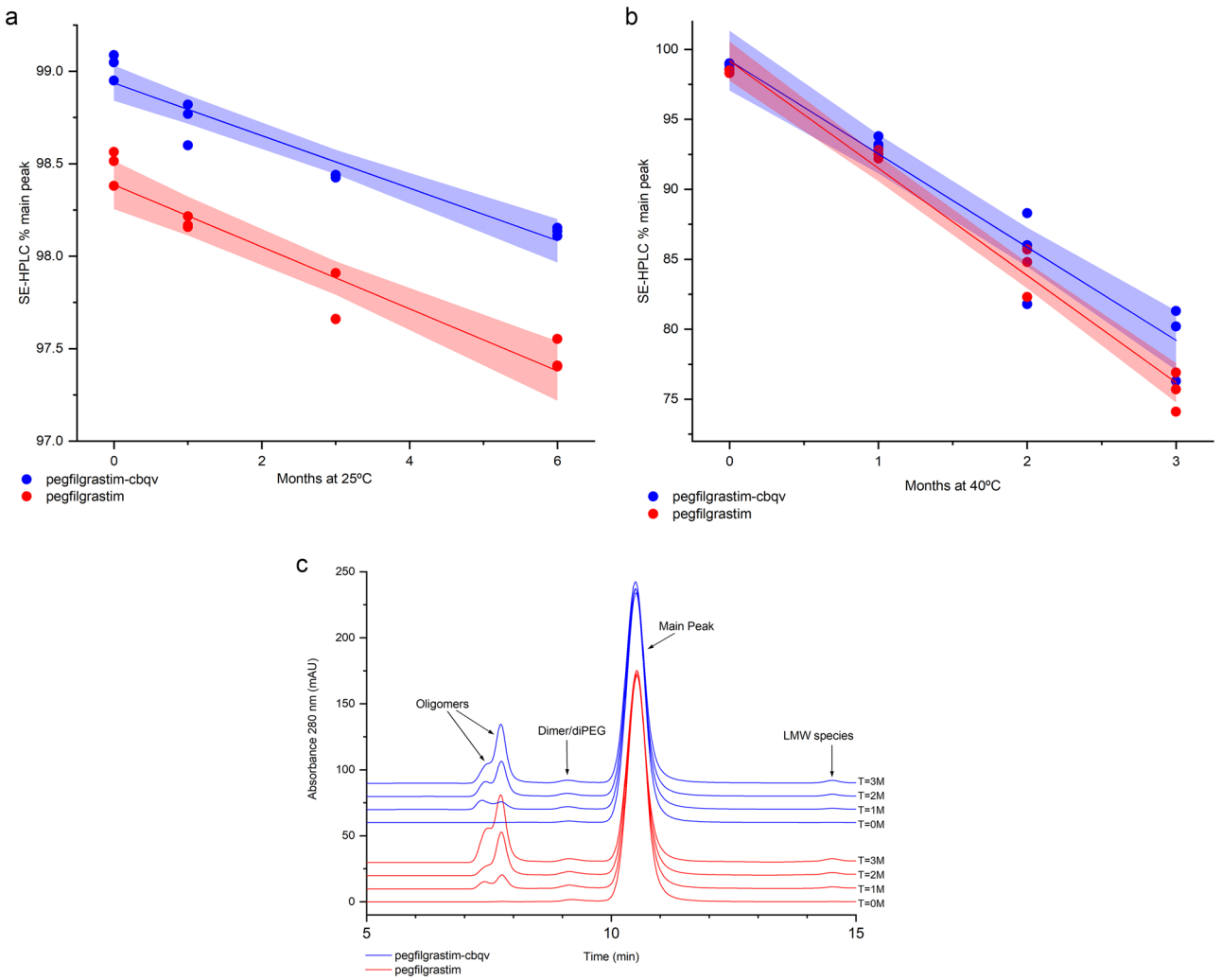

Fig. 8 SE-HPLC results from comparative stability studies of pegfilgrastim-cbqv to pegfilgrastim **a** change in SE-HPLC main peak at 25 °C, shaded areas show 95% confidence intervals of the fit; **b** changes in SE-HPLC at 40 °C, shaded areas show 95% confidence intervals of the fit; and **c** SE-HPLC chromatograms of pegfilgrastim-cbqv and pegfilgrastim subjected to stress conditions (40 °C for up to 3 months). *SE-HPLC* size-exclusion high-performance liquid chromatography

silicone oil droplets, which are spherical, a morphological filter was applied to report particles with aspect ratio <0.85. Particle concentrations for pegfilgrastim-cbqv and pegfilgrastim are compared in Table 1. Overall counts were variable but consistently higher in pegfilgrastim than in pegfilgrastim-cbqv.

3.5.2 Strength

Protein concentrations of pegfilgrastim-cbqv and pegfilgrastim lots were measured using UV spectroscopy. The concentration values were compared using an equivalence test with unequal variances. Variances were shown to be unequal by Levene's test [22]. The protein concentrations of pegfilgrastim-cbqv and pegfilgrastim were found to be equivalent (Table 1).

3.6 Comparative Stability

Comparable stability profiles are considered additional evidence of similarity between biosimilar and reference products. The stability of pegfilgrastim-cbqv and pegfilgrastim under accelerated (25 °C) and heat stressed (40 °C) storage conditions are presented here. A plot of SE-HPLC main peak decline over time is shown for 25 °C (Fig. 8a) and 40 °C (Fig. 8b) storage. Quantitative results and regression analyses are provided (Online Resource 1). The initial purity of pegfilgrastim-cbqv is higher on average than pegfilgrastim, causing the trend lines to be offset. However, the degradation rates (slopes) are similar for both conditions. Representative SE-HPLC chromatograms for pegfilgrastim-cbqv and pegfilgrastim heat stressed show comparable degradation profiles

(Fig. 8c). Aggregation was the primary mode of degradation detected by SE-HPLC for both materials.

4 Discussion

The totality of data generated by structural and functional methods, as well as comparative stability studies, support a conclusion of biosimilarity between pegfilgrastim-cbqv and its reference product, pegfilgrastim.

The primary structure of pegfilgrastim is more complex than most biosimilars, in that it encompasses a protein and a PEG moiety, connected by a molecular linker. In addition, the PEG portion of the molecule features polydispersity, which can vary depending on the PEG source lot. Primary structure results demonstrate that pegfilgrastim-cbqv and pegfilgrastim have identical amino-acid sequences and disulfide bonds. In addition, the main PEG attachment site, occupancy, and linker composition were shown to be the same for both products. Intact mass was higher for the pegfilgrastim-cbqv lots evaluated. The intact mass observed was consistent between all pegfilgrastim-cbqv and all pegfilgrastim lots. Given the possibility that a single lot of PEG may be used in production for several years, all lots of pegfilgrastim evaluated herein may be associated with a single lot of PEG. Similarly, all lots of pegfilgrastim-cbqv tested trace back to a single PEG lot. The differences observed did not translate into any difference in PK.

Higher-order structure results show consistent secondary and tertiary folding, as well as surface accessibility, between pegfilgrastim-cbqv and pegfilgrastim. Functional properties were demonstrated to be similar in both binding and cell-based methods. General attributes of pegfilgrastim-cbqv and pegfilgrastim, such as protein concentration, were demonstrated to be the same within method variability.

Variants in pegfilgrastim-cbqv and pegfilgrastim were compared using one-sided quality ranges, since lower variant content is acceptable in a biosimilar product. DiPEG species by CEC are slightly larger in pegfilgrastim-cbqv and the acceptance criterion was not met for diPEG species. The differences in diPEG pattern in pegfilgrastim-cbqv and pegfilgrastim may be due to minor differences in both the PEGylation and purification steps of the respective production processes. DiPEG variants were well under 1% for both pegfilgrastim-cbqv and reference product, and no clinical impact resulted from these minor differences [9, 10].

Pegfilgrastim-cbqv showed lower content of oxidized and deamidated species, as well as dimer by SE-HPLC. Subvisible particulates met the one-sided quality range, with higher numbers observed in the reference product. As dimer, oxidized and deamidated species, and subvisible particulates can be stability-indicating, it is possible that the product age at the time of testing contributed to the offset. While the reference product was within its expiration period at the time of testing, the date of manufacture is not available for pegfilgrastim lots; therefore, it is possible that the pegfilgrastim lots were older when tested. Stress stability studies showed comparable rates of degradation between pegfilgrastim-cbqv and pegfilgrastim.

5 Conclusions

The comparative analytical assessment of pegfilgrastim-cbqv to its reference product pegfilgrastim presented herein demonstrates that pegfilgrastim-cbqv is highly similar to pegfilgrastim. Analytical similarity was demonstrated through a totality of data, including a comprehensive structural and functional assessment. Minor differences in PEG molar mass and PEGylation variants did not affect functional activity and are not expected to impact the clinical efficacy of pegfilgrastim-cbqv. The analytical similarity of pegfilgrastim-cbqv to pegfilgrastim demonstrated in this comparative analytical assessment is consistent with clinical results where the two products were found to act equivalently [9, 10].

Supplementary Information The online version contains supplementary material available at https://doi.org/10.1007/s40268-024-00471-9.

Declarations

Funding This study was funded by Coherus BioSciences, Inc.

Conflicts of Interest All authors except M.M., E.V., B.A., and D.D. are current employees of Coherus BioSciences. At the time of the study, all authors were employees of Coherus BioSciences.

Ethics Approval Not applicable.

Consent to Participate Not applicable.

Consent for Publication Not applicable.

Data Availability Statement Data have been provided in Supplemental Materials. Coherus BioSciences will review all requests for additional data and consider providing those on a case-by-case basis.

Author Contributions The main text of the paper was written by H.K., J.D., and K.M. All authors contributed to the collection and analysis of data. All authors reviewed and approved the final manuscript.

References

1. Mulcahy A, Buttorff C, Finegold K, El-Kilani Z, Oliver JF, Murphy S, Jessup A. Projected US savings from biosimilars, 2021–2025. Am J Manag Care. 2022;28:329–35. https://doi.org/10.37765/ajmc.2022.88809.
2. US Food and Drug Administration. Scientific considerations in demonstrating biosimilarity to a reference product. Guidance for industry. https://www.fda.gov/regulatory-information/search-fda-guidance-documents/scientific-considerations-demonstrating-biosimilarity-reference-product Accessed 15 Mar 2024.
3. US Food and Drug Administration. Quality considerations in demonstrating biosimilarity of a therapeutic protein product to a reference product. Guidance for industry. https://www.fda.gov/regulatory-information/search-fda-guidance-documents/quality-considerations-demonstrating-biosimilarity-therapeutic-protein-product-reference-product Accessed 15 Mar 2024.
4. US Food and Drug Administration. Development of therapeutic protein biosimilars: comparative analytical assessment and other quality-related considerations. Guidance for industry. https://www.fda.gov/regulatory-information/search-fda-guidance-documents/development-therapeutic-protein-biosimilars-comparative-analytical-assessment-and-other-quality. Accessed 15 Mar 2024
5. Coherus Biosciences. UDENYCA® sales data up to October 2023.
6. Cost comparison of Wholesale Acquisition Cost (WAC) for UDENYCA® https://assets.website-files.com/655b7369762c6bc9dc66f15d/659de0550bbf83eebcc53291_doc-product-fact-sheet.pdf Accessed 18 Mar 2024 and Neulasta® https://www.neulasta.com/paying-for-neulasta. Accessed 18 Mar 2024.
7. Coherus Biosciences Inc. FDA Approves UDENYCA® Autoinjector. In: FDA Approves UDENYCA® Autoinjector. 2023. https://investors.coherus.com/news-releases/news-release-details/fda-approves-udenycar-autoinjector. Accessed 15 Mar 2024.
8. Coherus Biosciences. Coherus announces FDA approval of UDENYCA ONBODY™, a novel and proprietary state-of-the-art delivery system for pegfilgrastim-cbqv. 2024. https://investors.coherus.com/news-releases/news-release-details/coherus-announces-us-launch-udenyca-onbodytm-novel-and Accessed 15 Mar 2024.
9. Finck B, Tang H, Civoli F, Hodge J, O'Kelly H, Vexler V. Pharmacokinetic and pharmacodynamic equivalence of pegfilgrastim-cbqv and pegfilgrastim in healthy subjects. Adv Ther. 2020;37:4291–307. https://doi.org/10.1007/s12325-020-01459-y.
10. Civoli F, Finck B, Tang H, Hodge J, O'Kelly H, Vexler V. Biosimilar pegfilgrastim-cbqv demonstrated similar immunogenicity to pegfilgrastim in healthy subjects across three randomized clinical studies. Adv Ther. 2022;39:1230–46. https://doi.org/10.1007/s12325-021-02024-x.
11. Tsong Y, Dong X, Shen M. Development of statistical methods for analytical similarity assessment. J Biopharm Stats. 2017;27(2):197–205. https://doi.org/10.1080/10543406.2016.1272606.
12. Huang L. Characterization of poly(ethylene glycol) and PEGylated products by LC/MS with postcolumn addition of amines. Anal Chem. 2009;81:567–77.
13. Forstenlehner IC, Holzmann J, Scheffler K, Wieder W, Toll H, Huber CG. A direct-infusion- and HPLC-ESI-Orbitrap-MS approach for the characterization of intact PEGylated proteins. Anal Chem. 2014;86:826–34. https://doi.org/10.1021/ac403390y.
14. Mori S, Bath HG. Molecular-weight-sensitive detectors. In: Size exclusion chromatography. Molecular-weight-sensitive detectors. Berlin: Springer; 1999. p. 115–29.
15. Guerra PI, Acklin C, Kosky AA, Davis JM, Treuheit MJ, Brems DN. PEGylation prevents the N-terminal degradation of megakaryocyte growth and development factor. Pharm Res. 1998;15:1822–7. https://doi.org/10.1023/a:1011945704248.
16. Arvedson T, O'Kelly J, Yang BB. Design rationale and development approach for pegfilgrastim as a long-acting granulocyte colony-stimulating factor. BioDrugs. 2015;29:185–98. https://doi.org/10.1007/s40259-015-0127-4.
17. Lu HS, Fausset PR, Narhi LO, Horan T, Shinagawa K, Shimamoto G, Boone TC. Chemical modification and site-directed mutagenesis of methionine residues in recombinant human granulocyte colony-stimulating factor: effect on stability and biological activity. Arch Biochem Biophys. 1999;362:1–11. https://doi.org/10.1006/abbi.1998.1022.
18. Holzmann J, Hausberger A, Rupprechter A, Toll H. Top-down MS for rapid methionine oxidation site assignment in filgrastim. Anal Bioanal Chem. 2013;405:6667–74. https://doi.org/10.1007/s00216-013-7138-0.
19. Riggs DL, Silzel JW, Lyon YA, Kang AS, Julian RR. Analysis of glutamine deamidation: products, pathways, and kinetics. Anal Chem. 2019;91:13032–8. https://doi.org/10.1021/acs.analchem.9b03127.
20. Shekhawat R, Shah CK, Patel A, Srinivasan S, Kapoor P, Patel S, Kumar S, Sonar S, More N, Joshi M, et al. Structural similarity, characterization of poly ethylene glycol linkage and identification of product related variants in biosimilar pegfilgrastim. PLoS ONE. 2019;14: e0212622. https://doi.org/10.1371/journal.pone.0212622.
21. Akbarzadehlaleh P, Mirzaei M, Mashahdi-Keshtiban M, Heidari HR. The effect of length and structure of attached polyethylene glycol chain on hydrodynamic radius, and separation of PEGylated human serum albumin by chromatography. Adv Pharm Bull. 2021;11:728–38. https://doi.org/10.34172/apb.2021.082.
22. Levene H. Robust tests for equality of variances. In: Olkin I, Ghurye S, Hoeffding W, Madow WG, Mann HB, editors. Contributions to probability and statistics. Robust tests for equality of variances. Essays in Honor of Harold Hotelling. Stanford: Stanford University Press; 1960. p. 278–92.

Authors and Affiliations

Henriette Kuehne[1] · Janice M. Davis[1] · LeeAnne Merewether[1] · Matthew McQueen[1,2] · Elizabeth Valentine[1,3] · Glen Young[1] · Benjamin T. Andrews[1,4] · Dimitri Diaz[1,2] · Karen J. Miller[1]

✉ Karen J. Miller
kmiller@coherus.com

[1] Coherus BioSciences Inc., 1000 Avenida Acaso, Camarillo, CA 93012, USA

[2] Present Address: Avidity Biosciences, Inc., San Diego, CA, USA

[3] Present Address: Halozyme Therapeutics, San Diego, CA, USA

[4] Present Address: Genentech Inc., South San Francisco, CA, USA